Report
R-24-15
December 2024

Verification of a model for calculating the dilute water penetration in fractured rock – a MATLAB implementation

Pirouz Shahkarami

SVENSK KÄRNBRÄNSLEHANTERING AB

SWEDISH NUCLEAR FUEL
AND WASTE MANAGEMENT CO

Box 3091, SE-169 03 Solna
Phone +46 8 459 84 00
skb.se

SVENSK KÄRNBRÄNSLEHANTERING

ISSN 1402-3091
SKB R-24-15
ID 2065821
December 2024

Verification of a model for calculating the dilute water penetration in fractured rock – a MATLAB implementation

Pirouz Shahkarami, Kemakta Konsult AB

Summary

This report presents the verification of a MATLAB-based implementation of an analytical model for simulating solute transport through flow channels, stagnant water zones, and diffusion into adjacent rock matrices. The model is used to identify canister positions exposed to dilute water concentrations that could lead to buffer erosion. A detailed derivation of the model's analytical solution in the Laplace domain is provided alongside its introduction. This derivation ensures clarity and serves as a basis for verifying the solution. Additionally, a dedicated section of the report outlines the structure and workflow of the code package, providing guidance on generating or modifying new and existing cases. This includes altering geometrical dimensions, transport parameters, initial and boundary conditions, and pathway characteristics.

The model's accuracy was verified through a series of tests, comparing the MATLAB implementation with an equivalent Python implementation and, where applicable, results from the numerical model DarcyTools. The first numerical test disregarded the effect of the stagnant water zone, while the second included it. In both cases, the implementations showed excellent agreement. The third test assessed the fraction of deposition hole positions, being subject to dilute conditions, defined as a concentration of three percent of the initial value.

The successful completion of the verification tests, along with the derivation of the analytical solution and detailed guidance on the code workflow, helps to build confidence in the model and its implementation for safety assessment of radioactive waste repositories.

Sammanfattning

Denna rapport presenterar verifieringen av en MATLAB-baserad implementering av en analytisk modell för simulering av transport av lösta ämnen genom flödeskanaler, stagnanta vattenzoner och diffusion till intilliggande bergmatris. Modellen används för att identifiera kapselpositioner med jonsvaga vatten som kan leda till bufferterosion. En detaljerad härledning av modellens analytiska lösning i Laplace-domänen tillhandahålls tillsammans med en introduktion av modellen. Denna härledning säkerställer tydlighet och utgör en grund för verifiering av lösningen. Dessutom beskriver ett särskilt avsnitt i rapporten kodpaketets struktur och arbetsflöde, och ger vägledning i hur man genererar eller ändrar nya och befintliga beräkningsfall. Detta inkluderar ändring av geometriska dimensioner, transportparametrar, initial- och randvillkor samt egenskaper för flödesvägar.

Modellens noggrannhet verifierades genom en serie tester där MATLAB-implementeringen jämfördes med en likvärdig Python-implementering och, i förekommande fall, resultat från den numeriska modellen DarcyTools. Det första numeriska testet bortsåg från effekten av den stagnanta vattenzonen, medan det andra testet inkluderade den. I båda fallen visade implementeringarna utmärkt överensstämmelse. Det tredje testet utvärderade andelen av deponeringshålpositioner som uppnådde förhållanden med jonsvaga vatten, definierade som en koncentration av tre procent av det initiala värdet.

Det framgångsrika slutförandet av verifieringstesterna, tillsammans med härledningen av den analytiska lösningen och den detaljerade vägledningen om kodens arbetsflöde, bidrar till att stärka förtroendet för modellen och dess användning inom säkerhetsanalysen av ett förvar för radioaktivt avfall.

Contents

1 Introduction

SKB (2022) reports on radionuclide transport modelling for the post-closure safety assessment in support of SKB's Preliminary Safety Assessment Report (PSAR) for a final repository for spent nuclear fuel at the Forsmark site. Appendix K of (SKB, 2022) briefly describes the solute transport model developed by Mahmoudzadeh et al. (2013), which provides a framework for calculating the concentration of a non-decaying solute as it moves through the flow channel while accounting for the retarding effects of finite matrices and stagnant water zones adjacent to the flow channel (collectively referred to as "subsystems" in this report). The original solution by Mahmoudzadeh et al. (2013) assumes a zero-concentration initial condition within these subsystems. To meet the objectives of this study – namely, identifying canister positions exposed to dilute water concentrations that may lead to buffer erosion – the model has been modified to incorporate a non-zero initial condition. This adaptation enables the model to evaluate the impact of low-ionic-strength water infiltrating from the surface on salinity levels at repository depth. Specifically, the model determines the temporal distribution of deposition hole positions that reach a predefined concentration threshold. The necessary transport data for this analysis are derived from flow simulations conducted using ConnectFlow. This report provides a complete derivation of the analytical solution and verifies the MATLAB implementation of the solution.

The report is structured as follows: Section 2 provides a conceptual model of the solute transport mechanisms; Section 3 presents the mathematical model, including detailed discussions on solute transport through various mediums; Section 4 presents the solution for the mediums in the Laplace domain; Section 5 outlines the verification process, highlighting three specific tests conducted to assess the model's accuracy; and Section 6 details the code package structure and workflow, offering guidance on how to create and modify new and existing cases. References are provided at the end of the report for further reading.

2 Conceptual model

Groundwater in fractured bedrock primarily flows through conductive parts of the fractures, known as channels. These channels can intersect, forming a connected network of transport pathways throughout the bedrock. In contrast, the surrounding rock matrix is typically much less permeable, and transport in this region is generally dominated by molecular diffusion. To effectively model solute transport in these networks, it is essential to consider the different mechanisms influencing solute movement within each individual channel. In this study, we adopt a simplified model that uses a straight channel with a constant aperture and width. Figure 2-1 shows the conceptual picture of the model developed by Mahmoudzadeh et al. (2013), where water flows through a channel of width and aperture of $2W_f$ and $2b_f$, respectively. The adjacent stagnant water zone is assumed to be a rectangular cuboid with the same length as the flow channel but with a different aperture, $2b_s$, and width, $2W_s$. The flow velocity, u, is assumed to be uniform through the flow channel, and complete mixing across the fracture is assumed. Transport along the fracture is controlled by advection, while the effects of longitudinal dispersion are neglected in this study. Solutes can diffuse directly from (and to) the flow channel to (and from) the adjacent rock matrix. Alternatively, they may first diffuse into the stagnant water zone before moving into the rock matrix, and vice versa. Although, in Figure 2-1, diffusion to the stagnant water zone and rock matrices is shown in positive directions, the model also considers the diffusion in opposite directions. Solute is also subject to linear equilibrium sorption on the fracture surface and within the porous rock matrix. In this study, radioactive decay is not considered.

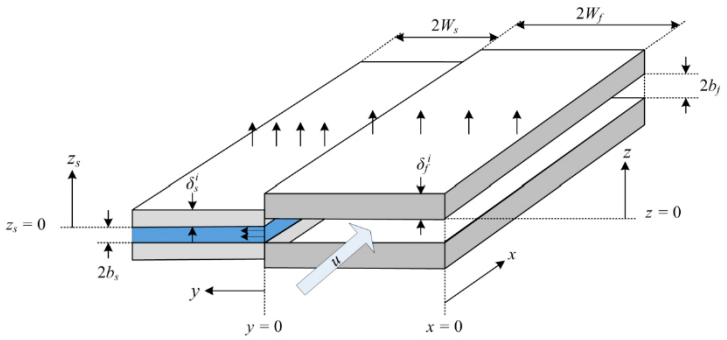

Figure 2-1. *Different paths for solute transport in fractured rock where solute diffuses to the stagnant water zone (denoted as the blue zone in the figure) and rock matrices in both positive and negative directions, after Mahmoudzadeh et al. (2013).*

3 Mathematical model

Solute transport can be described with the coupled one-dimensional approach, as was done by Mahmoudzadeh et al. (2013). Because the system has been conceptualized into four subsystems, four mass balance equations are formulated to describe transport in the flow channel, stagnant water zone, rock matrix adjacent to the flow channel and rock matrix adjacent to the stagnant water zone, respectively. To provide the coupling between the subsystems, solute exchange at the interfaces is described by introducing sink and source terms in the governing equations and by providing continuity of the concentration near the interfaces. The following sections present the system of equations that describe solute transport in each subsystem.

In each section, the process begins with the presentation of the transport equation, where the initial concentration in each subsystem is given as $C = C_0$. This form represents the model of solute transport considering the initial non-zero concentration. Following the introduction of this equation, a *change of variable* is applied to simplify the problem. Specifically, the transformed concentration $\tilde{C} = C - C_0$ is introduced. This transformation shifts the initial concentration to zero across all subsystems, allowing for an analytical approach (the Laplace transformation) to solve the transport equations. The *modified* equations are then presented, demonstrating how the system is now expressed in terms of the modified variable.

3.1 Solute transport through the flow channel

Based on the above considerations and by taking diffusive transport and linear equilibrium sorption into account, the one-dimensional transport equation of species *i* in the flow channel can be formulated as:

$$R_{f,i}\frac{\partial C_{f,i}}{\partial t} + u\frac{\partial C_{f,i}}{\partial x} = \frac{b_s}{b_f}\frac{D_{s,i}}{W_f}\frac{\partial C_{s,i}}{\partial y}\bigg|_{y=0} + \frac{D_{ef,i}}{b_f}\frac{\partial C_{pf,i}}{\partial z}\bigg|_{z=0} \tag{3-1}$$

In the above equation, x denotes the coordinate along the flow channel and y and z are the coordinates into the stagnant water zone and into the rock matrix adjacent to the flow channel, respectively; both are perpendicular to the channel. The terms on the right-hand side of the equation describe the diffusional process at the interfaces between the channel and the stagnant water zone and between the channel and the rock matrix adjacent to it, respectively. The initial condition is

$$C_{f,i}(x, 0) = C_0 \tag{3-2}$$

and boundary condition is given by:

$$C_{f,i}(0, t) = C_{in} \tag{3-3}$$

Upon introducing the following change of variable

$$\tilde{C}_{f,i} = C_{f,i} - C_0 \tag{3-4}$$

the transport equation and initial and boundary conditions becomes:

$$R_{f,i}\frac{\partial \tilde{C}_{f,i}}{\partial t} + u\frac{\partial \tilde{C}_{f,i}}{\partial x} = \frac{b_s}{b_f}\frac{D_{s,i}}{W_f}\frac{\partial \tilde{C}_{s,i}}{\partial y}\bigg|_{y=0} + \frac{D_{ef,i}}{b_f}\frac{\partial \tilde{C}_{pf,i}}{\partial z}\bigg|_{z=0} \tag{3-5}$$

$$\tilde{C}_{f,i}(x, 0) = 0 \tag{3-6}$$

$$\tilde{C}_{f,i}(0, t) = C_{in} - C_0 \tag{3-7}$$

3.2 Solute transport in the stagnant water zone

Neglecting diffusion in the direction parallel to the flow, the one-dimensional transport equation of species *i* in the stagnant water zone can be formulated as:

$$R_{s,i}\frac{\partial C_{s,i}}{\partial t} = D_{S,i}\frac{\partial^2 C_{s,i}}{\partial y^2} + \frac{D_{es,i}}{b_s}\frac{\partial C_{ps,i}}{\partial z_s}\bigg|_{z_s=0} \tag{3-8}$$

where z_s is the coordinate along the rock matrix adjacent to the stagnant water zone, and it is perpendicular to the interface between the stagnant water zone and the adjacent rock matrix. Here we neglect the diffusion in z_s direction within the stagnant water zone, assuming complete mixing across the thin fracture. The initial condition is

$$C_{s,i}(y,0) = C_0 \tag{3-9}$$

and boundary conditions are given by:

$$C_{s,i}(0,t) = C_{f,i} \tag{3-10}$$

and

$$\frac{\partial C_{s,i}}{\partial y}\bigg|_{y=2W_s} = 0 \tag{3-11}$$

The second term at the right-hand side of Equation (3-8) describes diffusion at the interface between the stagnant water zone and the rock matrix adjacent to it. Because complete mixing is assumed across the fracture, solute transport in the flow channel and in the stagnant water zone is coupled through Equation (3-10), which describes the continuity of the solute concentration at the interface. Equation (3-11) shows a no-flux boundary condition at $y = 2W_s$ in the stagnant water zone. The no-flux condition can be motivated as a symmetry condition with the neighbouring water zone in which transport occurs simultaneously. It may also be a physical boundary. Upon introducing the following change of variable:

$$\tilde{C}_{s,i} = C_{s,i} - C_0 \tag{3-12}$$

The transport equation and initial and boundary conditions becomes:

$$R_{s,i}\frac{\partial \tilde{C}_{s,i}}{\partial t} = D_{S,i}\frac{\partial^2 \tilde{C}_{s,i}}{\partial y^2} + \frac{D_{es,i}}{b_s}\frac{\partial \tilde{C}_{ps,i}}{\partial z_s}\bigg|_{z_s=0} \tag{3-13}$$

$$\tilde{C}_{s,i}(y,0) = 0 \tag{3-14}$$

$$C_{s,i}(0,t) = C_{f,i} - C_0 = \tilde{C}_{f,i} \tag{3-15}$$

$$\frac{\partial \tilde{C}_{s,i}}{\partial y}\bigg|_{y=2W_s} = 0 \tag{3-16}$$

3.3 Solute transport in the rock matrix adjacent to the flow channel

Transport in the porous rock matrix is primarily controlled by molecular diffusion, as the rock matrix usually has a very low hydraulic conductivity. The one-dimensional transport equation of species *i* in the matrix adjacent to the flow channel can be formulated as

$$R_{pf,i}\frac{\partial C_{pf,i}}{\partial t} = \frac{D_{ef,i}}{\varepsilon_{pf}}\frac{\partial^2 C_{pf,i}}{\partial z^2} \tag{3-17}$$

The initial condition is

$$C_{pf,i}(z,0) = C_0 \tag{3-18}$$

and the boundary conditions are given by:

$$C_{pf,i}(0,t) = C_{f,i} \tag{3-19}$$

and

$$\left.\frac{\partial \mathrm{C}_{pf,i}}{\partial \mathrm{z}}\right|_{z=\delta_f} = 0 \tag{3-20}$$

Because concentration does not vary across the fracture, transport in the flow channel and matrix is coupled through Equation (3-19), which describes the continuity of the solute concentration. Equation (3-20) describes a no-flux boundary condition at $z = \delta_f$ for a rock matrix adjacent to the flow channel. The rock matrix extends for a limited distance where no flux is permitted. The no-flux condition can be motivated as a symmetry condition with a neighbouring matrix in which transport occurs simultaneously. When a large value is used for the matrix depth, the matrix may act as a semi-infinite domain with infinite fracture spacing. Upon introducing the following change of variable:

$$\tilde{C}_{pf,i} = C_{pf,i} - C_0 \tag{3-21}$$

The transport equation and initial and boundary conditions becomes:

$$R_{pf,i}\frac{\partial \tilde{C}_{pf,i}}{\partial t} = \frac{D_{ef,i}}{\varepsilon_{pf}}\frac{\partial^2 \tilde{C}_{pf,i}}{\partial z^2} \tag{3-22}$$

$$\tilde{C}_{pf,i}(z,0) = 0 \tag{3-23}$$

$$\tilde{C}_{pf,i}(0,t) = C_{f,i} - C_0 = \tilde{C}_{f,i} \tag{3-24}$$

$$\left.\frac{\partial \tilde{C}_{pf,i}}{\partial z}\right|_{z=\delta_f} = 0 \tag{3-25}$$

3.4 Solute transport in the rock matrix adjacent to the stagnant water zone

Similar to Equation (3-17), the one-dimensional transport equation of species *i* in the rock matrix adjacent to the stagnant water zone can be formulated as:

$$R_{ps,i}\frac{\partial C_{ps,i}}{\partial t} = \frac{D_{es,i}}{\varepsilon_{ps}}\frac{\partial^2 C_{ps,i}}{\partial z_s^2} \tag{3-26}$$

The initial condition is

$$C_{ps,i}(z_s,0) = C_0 \tag{3-27}$$

and boundary conditions are given by:

$$C_{ps,i}(0,t) = C_{s,i} \tag{3-28}$$

and

$$\left.\frac{\partial C_{ps,i}}{\partial z_s}\right|_{z_s=\delta_s} = 0 \tag{3-29}$$

Equation (3-28) describes the continuity of concentration between the stagnant water zone and its adjacent rock matrix. Equation (3-29) also describes a no-flux boundary condition at $z_s = \delta_s$ for the rock matrix adjacent to the stagnant water zone. Upon introducing the following change of variable:

$$\tilde{C}_{ps,i} = C_{ps,i} - C_0 \tag{3-30}$$

The transport equation and initial and boundary conditions becomes:

$$R_{ps,i}\frac{\partial \tilde{C}_{ps,i}}{\partial t} = \frac{D_{es,i}}{\varepsilon_{ps}}\frac{\partial^2 \tilde{C}_{ps,i}}{\partial z_s^2} \tag{3-31}$$

$$\tilde{C}_{ps,i}(z_s, 0) = 0 \tag{3-32}$$

$$\tilde{C}_{ps,i}(0, t) = C_{s,i} - C_0 = \tilde{C}_{s,i} \tag{3-33}$$

$$\left.\frac{\partial \tilde{C}_{ps,i}}{\partial z_s}\right|_{z_s=\delta_s} = 0 \tag{3-34}$$

4 Solution in the Laplace Domain

In this section, we begin with the Laplace transformed solutions to transport equations in the rock matrices and then continue with the equations describing solute transport in the stagnant water zone and the flow channel. The solutions are obtained for the *modified* equations and are expressed according to the parameter groups introduced by Mahmoudzadeh et al. (2013), which help to characterise the mechanisms contributing to solute transport. These parameter groups together with their definitions and physical significance are listed in Table 4-1.

Table 4-1. Parameter groups used to characterize the transport equations.

Definition	Physical Significance
$MPG_{pf} = \sqrt{D_{ef} R_{pf} \varepsilon_{pf}}$	Material property group for the rock matrix adjacent to the flow channel (Moreno and Crawford, 2009).
$MPG_{ps} = \sqrt{D_{es} R_{ps} \varepsilon_{ps}}$	Material property group for the rock matrix adjacent to the stagnant water zone (Moreno and Crawford, 2009).
$F_f = \frac{x}{u b_f}$	Ratio of the flow-wetted surface of the rock matrix adjacent to the flow channel to the advection conductance (volumetric water flow rate). F_f gives a measure of the ratio of diffusion through the rock matrix to advection in the flow channel and quantifies the relative importance of these two types of solute transport in the channel. A high value of the F_f indicates that a large amount of solute carried by the flowing water can quickly be transported into the rock matrix.
$F_s = \frac{{W_s}^2}{D_S . b_s}$	Ratio of the flow-wetted surface of the rock matrix adjacent to the stagnant water zone to the diffusion conductance of the stagnant water zone. F_s gives a measure of the ratio of diffusion through the rock matrix to diffusion into the stagnant water zone and quantifies the relative importance of these two types of solute transport. A high value of F_s indicates that a large amount of solute diffusing from the flow channel into the stagnant water zone can quickly be sucked by the rock matrix.
$\tau_f = \frac{x}{u}$	Characteristic time for advection through the flow channel, which is equivalent to the water residence time.
$\tau_s = \frac{{W_s}^2}{D_{S,i}}$	Characteristic time for diffusion into the stagnant water zone.
$\tau_{Df,i} = \frac{{\delta^2}_f}{D_{af,i}}$	Characteristic time for diffusion into the rock matrix adjacent to the flow channel.
$\tau_{Ds,i} = \frac{{\delta^2}_s}{D_{as,i}}$	Characteristic time for diffusion into the rock matrix adjacent to the stagnant water zone.
$N = \frac{D_S x b_s / W_s}{u b_f W_f}$	Ratio of the characteristic rate of diffusion into the stagnant water zone to the characteristic rate of advection through the flow channel. N gives a measure of the fraction of solutes that can depart from the flow channel into the stagnant water zone.

In the table above, $D_{af,i}$ and $D_{as,i}$ are the apparent diffusivity of species i within rock matrices adjacent to the flow channel and stagnant water zone, respectively, defined as.

$$D_{af,i} = \frac{D_{ef,i}}{\varepsilon_{pf} R_{pf,i}} \tag{4-1}$$

$$D_{as,i} = \frac{D_{es,i}}{\varepsilon_{ps} R_{ps,i}} \tag{4-2}$$

4.1 Solute transport through the rock matrix adjacent to the flow channel

We define *T* and *P* representing the Laplace-transformed concentrations in the flow channel and in the rock matrix adjacent to it, respectively, hence

$$T_i = L\left(\tilde{C}_{f,i}\right) \tag{4-3}$$

$$P_i = L\left(\tilde{C}_{pf,i}\right) \tag{4-4}$$

It follows that, the partial differential equation in the Laplace domain for solute transport through the rock matrix adjacent to the flow channel can be derived as:

$$\frac{\partial^2 P_i}{\partial z^2} - \frac{\tau_{Df,i} s}{\delta_f^2} P_i = 0 \tag{4-5}$$

where *s* denotes the Laplace transform variable. The Laplace-transformed boundary conditions become:

$$P_i(z = 0, s) = T_i \tag{4-6}$$

$$\left.\frac{\partial P_i}{\partial z}\right|_{z=\delta_f} = 0 \tag{4-7}$$

The general solution for this type of partial differential equations can be expressed as (Bird et al. 2002):

$$P_i = \beta_1 cosh\left(\frac{\sqrt{|\tau_{Df,i} s|}}{\delta_f}\left(z - \delta_f\right)\right) + \beta_2 sinh\left(\frac{\sqrt{|\tau_{Df,i} s|}}{\delta_f}\left(z - \delta_f\right)\right) \tag{4-8}$$

Applying the boundary conditions given in Equations (4-6) and (4-7), it can be shown that the final solution for solute transport equation in Laplace domain in rock matrix adjacent to flow channel can be obtained as:

$$P_i = \frac{T_i}{cosh\left(\sqrt{|\tau_{Df,i} s|}\right)} cosh\left(\frac{\sqrt{|\tau_{Df,i} s|}}{\delta_f}\left(z - \delta_f\right)\right) \tag{4-9}$$

Hence

$$\left.\frac{\partial P_i}{\partial z}\right|_{z=0} = -\frac{\sqrt{\tau_{Df,i}\, s}}{\delta_f} . Tanh\left(\sqrt{\tau_{Df,i}\, s}\right) \times T_i = \widetilde{\Psi}_i \times T_i \tag{4-10}$$

The above equation will be used later to solve the solute transport equation in the flow channel, Equation (4-26).

4.2 Solute transport through the rock matrix adjacent to the stagnant water zone

We define *H* and *E* representing the Laplace-transformed concentrations in the stagnant water zone and in the rock matrix adjacent to it, respectively, hence

$$H_i = L\left(\tilde{C}_{s,i}\right) \tag{4-11}$$

$$E_i = L\left(\tilde{C}_{ps,i}\right) \tag{4-12}$$

It follows that, the partial differential equation in the Laplace domain for solute transport through the rock matrix adjacent to the stagnant water zone can be derived as:

$$\frac{\partial^2 E_i}{\partial z_s^2} - \frac{\tau_{Ds,i} s}{\delta_s^2} E_i = 0 \tag{4-13}$$

with the Laplace-transformed boundary conditions:

$$E_i(z_s = 0, s) = H_i \tag{4-14}$$

$$\left.\frac{\partial E_i}{\partial z_s}\right|_{z_s=\delta_s} = 0 \tag{4-15}$$

The solution to the above transport equation can be obtained by following the same procedure used in Section 4.1. The final solution reads:

$$E_i = \frac{H_i}{Cosh\left(\sqrt{|\tau_{Ds,i} s|}\right)} Cosh\left(\frac{\sqrt{|\tau_{Ds,i} s|}}{\delta_s}(z_s - \delta_s)\right) \tag{4-16}$$

Hence

$$\left.\frac{\partial E_i}{\partial z_s}\right|_{z_s=0} = -H_i \times \frac{\sqrt{\tau_{Ds,i}\, s}}{\delta_s}.Tanh\left(\sqrt{\tau_{Ds,i}\, s}\right) \tag{4-17}$$

The above equation will be used later to solve the solute transport equation in the stagnant water zone, Equation (4-18).

4.3 Solute transport in the stagnant water zone

the Laplace-transformed form of Equation (3-13) for solute transport through the stagnant water zone can be derived as:

$$-W_s^2 \frac{\partial^2 H_i}{\partial y^2} = F_{s,i} D_{es,i} \left.\frac{\partial E_i}{\partial z_s}\right|_{z_s=0} - \tau_{S,i} R_{s,i} s H_i \tag{4-18}$$

with the Laplace-transformed boundary conditions:

$$H_i(y = 0, s) = T_i \tag{4-19}$$

$$\left.\frac{\partial H_i}{\partial y}\right|_{y=2W_s} = 0 \tag{4-20}$$

By substituting Equation (4-17) in Equation (4-18) we get:

$$\frac{\partial^2 H_i}{\partial y^2} - \frac{\tilde{g}_i}{W_s^2} H_i = 0 \tag{4-21}$$

Where $\tilde{g}_i$ is defined as:

$$\tilde{g}_i = F_{s,i} D_{es,i} \left(\frac{\sqrt{\tau_{Ds,i}\, s}}{\delta_s}.Tanh\left(\sqrt{\tau_{Ds,i}\, s}\right)\right) + \tau_{S,i} R_{s,i} s \tag{4-22}$$

The general solution for this type of differential equations can be expressed as:

$$H_i = \alpha_3 cosh\left(\frac{\sqrt{|\tilde{g}_i|}}{W_s}(y - 2W_s)\right) + \alpha_4 sinh\left(\frac{\sqrt{|\tilde{g}_i|}}{W_s}(y - 2W_s)\right) \quad (4\text{-}23)$$

Applying the boundary conditions given in Equations (4-19) and (4-20), it can be shown that the final solution for solute transport equation in Laplace domain in the stagnant water zone can be obtained as:

$$H_i = \frac{T_i}{cosh\left(2\sqrt{|\tilde{g}_i|}\right)} cosh\left(\frac{\sqrt{|\tilde{g}_i|}}{W_s}(y - 2W_s)\right) \quad (4\text{-}24)$$

Hence

$$\left.\frac{\partial H_i}{\partial y}\right|_{y=0} = -\frac{\sqrt{|\tilde{g}_{i,i}|}}{W_s} Tanh\left(2\sqrt{|\tilde{g}_{i,i}|}\right) \times T_i = \widetilde{\Phi}_i \times T_i \quad (4\text{-}25)$$

The above equation will be used later to solve the solute transport equation in the flow channel, Equation (4-26).

4.4 Solute transport through the flow channel

the Laplace-transformed form of Equation (3-5) for solute transport through the stagnant water zone can be derived as:

$$u\frac{\partial T_i}{\partial x} = \frac{b_s}{b_f}\frac{D_{s,i}}{W_f}\left.\frac{\partial H_i}{\partial y}\right|_{y=0} + \frac{D_{ef,i}}{b_f}\left.\frac{\partial P_i}{\partial z}\right|_{z=0} - R_{f,i}sT_i \quad (4\text{-}26)$$

with the Laplace-transformed boundary condition:

$$T_i(x = 0, s) = T_{in,i} - \frac{C_0}{s} \quad (4\text{-}27)$$

By substituting Equations (4-10) and (4-25) in Equation (4-26) we get:

$$u\frac{\partial T_i}{\partial x} = \tilde{s}_i \times T_i \quad (4\text{-}28)$$

Where $\tilde{s}_i$ is defined as:

$$\tilde{s}_i = a_{fs}D_{s,i}\widetilde{\Phi}_i + a_{fp}D_{ef,i}\widetilde{\Psi}_i - R_{f,i}s \quad (4\text{-}29)$$

In the above equation, a_{fs} and a_{fp} are flow wetted surface areas per volume of water for diffusion from flow channel to stagnant water zone and rock matrix, respectively, defined as:

$$a_{fs} = \frac{b_s}{b_f W_f} \quad (4\text{-}30)$$

and

$$a_{fp} = \frac{1}{b_f} \quad (4\text{-}31)$$

The general solution to Equation (4-28) (first-order linear constant coefficient ordinary differential equation) is in the form of (Bird et al. 2002):

$$T_i = r_{1,i} \times \exp\left(-\frac{|\tilde{s}_i|}{u}x\right) \quad (4\text{-}32)$$

Applying the boundary condition given in Equation (4-27), it can be shown that the final solution for solute transport equation in Laplace domain in the flow channel can be expressed as:

$$T_i = \left(T_{in,i} - \frac{C_0}{s}\right) \times \exp(-A_i) \tag{4-33}$$

Where A_i is defined as:

$$A_i = \frac{|\tilde{s}_i|x}{u} = \Omega_{f,i} + N_i \times \sqrt{\Omega_{s,i}} \times \ Tanh\left(2\sqrt{\Omega_{s,i}}\right) \tag{4-34}$$

in which we have defined $\Omega_{f,i}$ and $\Omega_{s,i}$ as:

$$\Omega_{f,i} = R_{f,i}\ \tau_{f,i} s + F_f P_{pf,i}\sqrt{s} \tag{4-35}$$

$$\Omega_{s,i} = R_{s,i}\tau_{s,i} s + F_{s,i} P_{ps,i}\sqrt{s} \tag{4-36}$$

with

$$P_{pf,i} = MPG_{pf,i} \times \ Tanh\left(\sqrt{\tau_{Df,i}\ s}\right) \tag{4-37}$$

$$P_{ps,i} = MPG_{ps,i} \times \ Tanh\left(\sqrt{\tau_{Ds,i}\ s}\right) \tag{4-38}$$

We have defined T as the Laplace transform of the modified concentration, therefore,

$$T_i = L\left(\tilde{C}_{f,i}\right) = L\left(C_{f,i} - C_0\right) = \ L\left(C_{f,i}\right) - \frac{C_0}{s} \tag{4-39}$$

hence

$$L\left(C_{f,i}\right) = \frac{C_0}{s} + \ \left(T_{in,i} - \frac{C_0}{s}\right) \times \exp(-A_i) \tag{4-40}$$

or equivalently:

$$L\left(C_{f,i}\right) = \frac{C_0}{s} \times [1 - \exp(-A_i)] + T_{in,i} \times \exp(-A_i) \tag{4-41}$$

Thus, the final solution is a function of solute concentration at the inlet boundary. By knowing the channel inlet condition, solute concentration along the flow channel, and through the other zones can be obtained by using the analytical expressions presented in the section. A complete list of characteristic parameters is given in Table 4-1 together with their definition and physical significance.

Equation (4-41) suggests that for practical applications, i.e., predicting the behaviour of solute transport in fractured media, one needs to follow the change in flow channels (solute particle pathways) and document the involved characteristic parameters, particularly τ_f and F_f. Such information is then sufficient to calculate the parameter A_i for each pathway and to obtain the solute concentration at the end of the path. The De Hoog algorithm can then be used to numerically invert Equation (4-41) back to the time domain. The algorithm is well described in (De Hoog et al., 1982) and briefly reviewed by Boupha et al. (2004).

In the case of fresh water at the inlet boundary ($C_{in} = 0$), the solution given in Equation (4-41) reduced to:

$$L\left(C_{f,i}\right) = \frac{C_0}{s} \times [1 - \exp(-A_i)] \tag{4-42}$$

For a simple case, where there is no stagnant water zone, $W_s = 0$, and the initial concentration in the subsystem is $C_0 = 0$, Equation (4-41) reduced to:

$$L\left(C_{f,i}\right) = T_{in,i} \times \exp\left(-R_{f,i}\ \tau_{f,i} s - F_f P_{pf,i}\sqrt{s}\right) \tag{4-43}$$

In this section, we presented the derivation of the analytical solution in the Laplace domain. In the following section, we proceed to verify the accuracy of this solution and its implementation in MATLAB. This step involves running numerical simulations using other tools to ensure that the MATLAB code correctly reproduces the analytical results, thereby verifying the computational approach.

5 Verification

This section focuses on the verification of the analytical solution and its implementation in MATLAB, against two alternative numerical models: 1) a Python implementation of the same analytical solution developed by Amphos21, and 2) the coupling of the numerical model DarcyTools (Svensson et al., 2010) with the Matrix Diffusion Module (MD Module) (Shahkarami and Sidborn, 2023).

5.1 Test 1 – Disregarding the effect of the stagnant water zone

In the first test, the MATLAB implementation was compared with both the Python script and DarcyTools, where the effect of stagnant water zone was disregarded. The verification phase involved evaluating the MATLAB implementation for two distinct cases, denoted Case 1 and Case 2, each defined by different values of τ_f (57 and 137 years, respectively) and F_{f+} (3.7×10^5 and 5.6×10^6 year/m, respectively). The remaining parameters were assumed to be constants and are summarized in Table 5-1.

Table 5-1. Geometrical and physical Properties of fracture and stagnant water used.

Parameter	Definition	Value
$\delta_f = \delta_s$	Half-size of matrix blocks	12.5 m
$\varepsilon_{pf} = \varepsilon_{ps}$	Matrix porosity	3.7×10^{-3}
$D_{ef} = D_{es}$	Effective diffusivity	4×10^{-14} m^2/s
D_s	Diffusivity in stagnant water zone	1×10^{-9} m^2/s
W_s	SWZ* Half width	1 m
C_{in}	Concentration of injected water	0.2 g/L
C_0	Concentration of initial fracture and matrix waters	10 g/L
W_f	Half-width of flow channel	0.1 m

* Stagnant Water Zone.

As shown in Figure 5-1, the test was completed successfully in both cases, demonstrating agreement across the three implementations. This agreement indicates that the implementations are consistent, thereby verifying the MATLAB implementation.

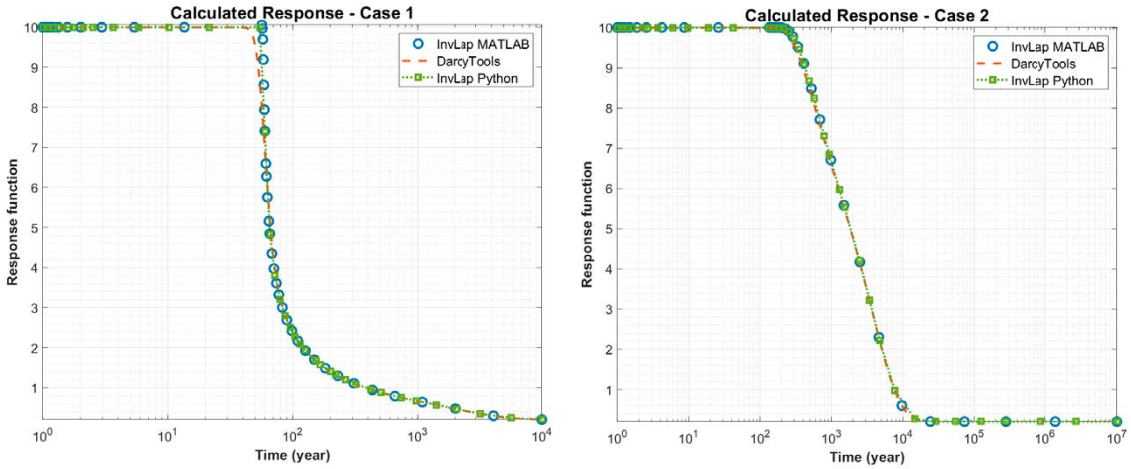

Figure 5-1. Comparison of responses from MATLAB, Python, and DarcyTools implementations in Case 1 (left) and Case 2 (right), where the effect of stagnant water zone was disregarded.

5.2 Test 2 – Including the effect of the stagnant water zone

A similar study was conducted that incorporated the effect of the stagnant water zone in the transport solution. This study involved a comparison between the MATLAB and Python implementations. It should be noted that the MD module in DarcyTools is designed to simulate diffusion within a single secondary continuum; thus, it cannot simultaneously model diffusion into or from both a rock matrix and a stagnant water zone. Consequently, DarcyTools was not used in this study, and the comparison was carried out between the MATLAB and Python implementations. The results for Case 1 and Case 2 are shown in Figure 5-2, which also demonstrate excellent agreement and indicates identical performance across the two implementations.

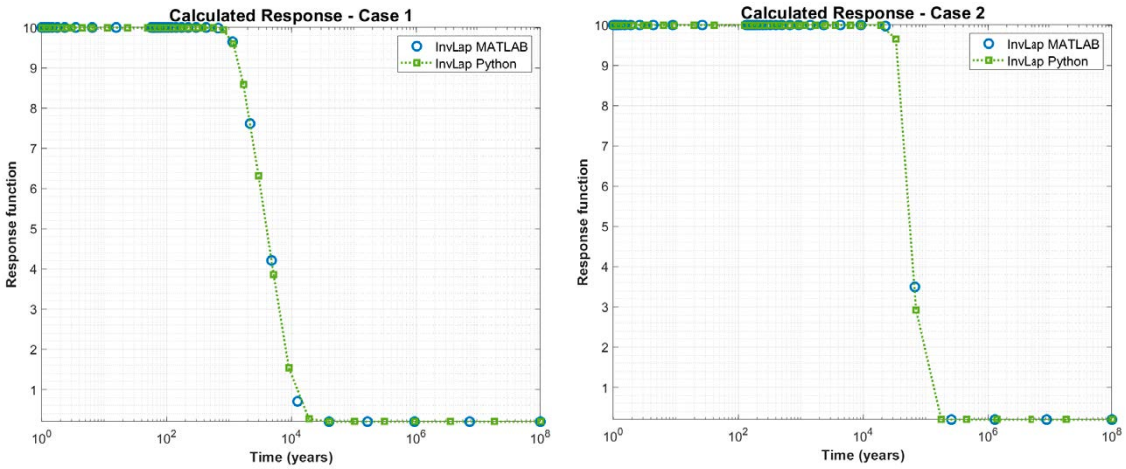

Figure 5-2. *Comparison of responses from MATLAB, Python, and DarcyTools implementations in Case 1 (left) and Case 2 (right), where the effect of stagnant water zone was included.*

5.3 Test 3 – Temporal distribution for deposition hole positions reaching three percent of the initial concentration

To strengthen the verification process, a comparison of the MATLAB and Python scripts was also conducted regarding the plots included in Appendix K of (SKB, 2022). Specifically, Figure K-5 (top) in the report was reproduced using both implementations and for $W_s = 0.1$, $W_s = 1.0$ and $W_s = 5.0$ m. The results, depicting the temporal distribution of deposition hole positions that reach three percent (3 %) of the initial concentration (10 g/L), are shown in Figure 5-3. The top left figure corresponds to $W_s = 0.1$ m, while the top right figure corresponds to $W_s = 1.0$ m, and the bottom left figure corresponds to $W_s = 5.$ m. The final figure presents an ensemble of all the cases (bottom right). It can be observed that the two implementations coincide in both cases, reproducing the same plot as reported in the SKB report. This agreement reinforces the notion that the implementations are consistent and robust, providing confidence in the ability of the MATLAB implementations to model the studied system.

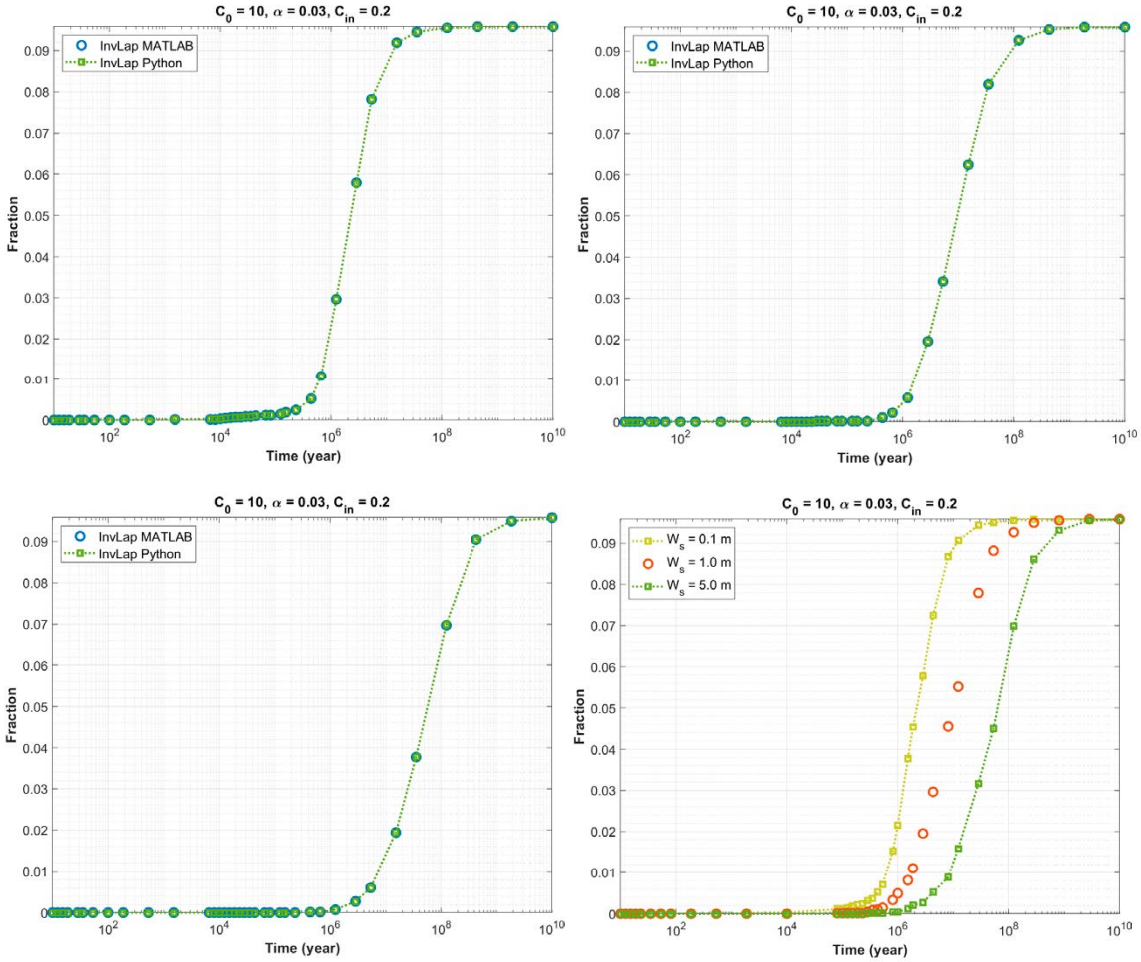

Figure 5-3. *Comparison of temporal distribution for all deposition hole positions that reach three percent of the initial concentration, for $W_s = 0.1$ (top left), $W_s = 1.0$ (top right), $W_s = 5.0$ m (bottom left), and an ensemble of all cases (bottom right).*

6 Code Package Structure and Workflow

6.1 Introduction

6.1.1 Purpose of the Code Package

The above formulations are implemented in MATLAB, and the accompanied code package is designed to handle various groundwater infiltration scenarios. It employs the De Hoog algorithm to perform the numerical inversion of the Laplace-transformed solution, Equation (4-41), back into the time domain, allowing for the analysis of multiple groundwater recharge pathways. Each pathway is characterized by unique values of F_f and τ_f. By calculating the concentration through these pathways, the code helps estimate the potential impact of dilute groundwater infiltration on canisters during temperate and glacial conditions.

6.1.2 Target Audience

To effectively use this code package, users are expected to have a basic familiarity with the MATLAB environment, including the ability to run scripts, navigate directories, and manage input/output files. However, users who wish to modify the code or simulate new cases must be comfortable with MATLAB programming and possess prior experience in coding. This includes understanding MATLAB's syntax, debugging capabilities, and working with functions and scripts.

6.2 Overview of Code Package Structure

6.2.1 Directory Structure

The code package is organized into a simple structure consisting of scripts, an input data file, and supporting resources for simulations. A sample directory layout is shown below:

/code_package

├── figures/

├── BasicSetting.m

├── invlap.m

├── Kopia av backward paths.xlsx

├── LPSolution.m

└── PSARcalculations.m

Below is a description of the main directory and its contents:

figures/: This folder contains a compilation of graphical outputs presenting the results, which are generated after simulations with varying parameters, i.e., W_f, W_s and α, where $\alpha = C/C_0$.

BasicSetting.m: A script used to define and configure the geometrical dimensions and transport parameters for the simulation environment. This includes initializing constants and setting up model characteristic parameters, as defined in Table 4-1.

LPSolution.m: This script processes the output from the previous script to calculate P_{pf} and P_{ps} as defined in Equations (4-37) and (4-38), respectively. These values are then utilized to construct the final core solution, described by Equation (4-41), in the Laplace domain. This solution is subsequently used by **invlap.m** for the numerical inversion of Laplace transforms into the time domain.

invlap.m: This script is used for the numerical inversion of Laplace transforms, allowing the simulation to move from the Laplace domain back to the time domain. The De Hoog algorithm, widely used for numerical inversion, is implemented here.

PSARcalculations.m: This script initiates and manages the overall simulation flow, focusing on the penetration of dilute water through various pathways. It starts with the initialization of model parameters and proceeds to read particle tracking data from the input .xlsx file. This file contains information on t_w, F_f, validation flags (OKFLAG), the full perimeter criterion (FPC), and effective full perimeter (EFPC). The last two parameters are criteria for exclusion of deposition holes. For example, excluding FPC > 0 means that deposition holes are excluded due to background fractures or deformation zone fractures. Please refer to (SKB, 2022) for further information regarding the particle tracking parameters. The script keeps desired deposition holes where OKFLAG(i) = 0, FPC(i) = 0, and EFPC(i) < 5, and calculates the outlet concentration of the dilute water for each path by recursively calling the function **invlap**. This iterative process ensures that the concentration profile is generated for each valid pathway. Next, the script identifies positions experiencing the erosion concentration[1] (C_{crit}) and computes the fraction of these positions. Finally, it plots the calculated fraction, exports the figure as a .png file, and concludes the simulation workflow.

6.3 Installation and Setup

To run this code package, the only prerequisites are having MATLAB installed and possessing a valid MATLAB license. There are no additional installation steps or specific setup procedures required. Once MATLAB is installed, users can simply download or clone the code package, navigate to the appropriate directory in MATLAB, and begin by running the script **PSARcalculations.m**. All necessary files, such as input data and scripts, are included in the package, so no further dependencies need to be installed to reproduce the existing cases.

6.4 Creating New Cases

To create new cases, users can modify various aspects of the provided scripts, input data and model parameters. Here's an overview of the different ways to create new cases, along with practical steps on how to implement them:

6.4.1 Modify geometrical dimensions and transport parameters

BasicSetting.m allows users to define essential model parameters, particularly for the stagnant water zone, the adjacent rock matrix, and the matrix adjacent to the fracture. These input parameters control the physical dimensions and transport properties of the subsystems, affecting the overall simulation. User-defined input parameters are:

1. **Fracture properties**
   - **Wf**: Fracture half-width. Default value: 0.1 m.
   - **FRf**: F_f for the fracture. Default value: provided by the user through input F year/m.
   - **Rf**: Retardation factor for the fracture. Default value: 1.0.
2. **Stagnant water zone properties**
   - **Ws**: Stagnant water zone half-width. Default value: 1.0 m.
   - **tw**: Water resistance time, defined by the user input TW year.
   - **bf**: Fracture half-aperture (m) computed as tw/FRf.
   - **Ds**: Water diffusivity in the stagnant water zone. Default value: 0.0315 m²/y.
   - **Rs**: Retardation factor in the stagnant water zone. Default value: 1.0. It can also be set to 0.0 if the stagnant water zone effect is neglected.
3. **Properties of matrix adjacent to the fracture**
   - **deltaf**: Penetration depths (m). Default value: 12.5 m.
   - **Def**: Effective diffusivity for the matrix adjacent to the fracture. Default value: 1.26×10^{-6} m²/y.
   - **KdfRbf**: Product of distribution coefficient (based upon the bulk density) and bulk density for the matrix. Default value: 4.0×10^{-5} (= ε_{pf}, hence, no sorption is considered within the rock matrix).

[1] Salinity criterion for buffer erosion, which represents the dilute water concentration at which buffer erosion may occur.

$$R_{pf}\varepsilon_{pf} = K_d\rho_p = \varepsilon_{pf} + \left(1 - \varepsilon_{pf}\right) \cdot K_d'\rho_s \quad (6\text{-}1)$$

K_d and K_d' are the matrix sorption coefficients based upon the bulk (ρ_p) and solid densities (ρ_s), respectively; ε_{pf} is the matrix porosity. The relation between the bulk and solid densities is:

$$\rho_p = \left(1 - \varepsilon_{pf}\right)\rho_s \quad (6\text{-}2)$$

4. **Properties of matrix adjacent to the stagnant water zone**
   - **deltas**: Penetration depths. Default value: 12.5 m.
   - **Des**: Effective diffusivity for the matrix adjacent to the stagnant water zone. Default value: 1.26×10^{-6} m²/y.
   - **KdsRbs**: Product of distribution coefficient (based upon the bulk density) and bulk density for the matrix. Default value: 4.0×10^{-5} (= ε_{pf}, hence, no sorption is considered within the rock matrix).

6.4.2 Alter initial and boundary conditions and simulation time

PSARcalculations.m can be adapted to simulate new cases by altering the initial condition, C_0, (Default value: 10 g/L), inlet concentration boundary, C_{in} (Default value: 0.2 g/L), α (Default value: 0.03) and hence C_{crit}, and simulation time.

6.4.3 Alter pathway characteristics from the input Excel file

Update the current or create a new Excel input file with different particle tracking data. Ensure to follow the same column structure given in the current file, keeping in mind that any data above row 11 is not used by the script.

6.4.4 Modify core equation in the Laplace domain

Update the core solution in **LPSolution.m** to create new cases that reflect new transport mechanisms or modified types of boundary conditions.

6.5 Input/Output Structure

The code package reads input data from an Excel file, which contains five (5) key columns necessary for the simulation. It's important to note that **any data above row 11 is not used by the script**, and the relevant data starts from row 11. The specific columns that are extracted and used in the simulation are column #M (τ_f), column #N (F_f) , column #I (OKFLAG), column #AB (FPC) and column #AC (EFPC).

The primary output of the code package is a MATLAB figure that visualizes the simulation results, such as concentration evolution over time for different pathways and the corresponding fraction of deposition holes that encounter dilute water with a specific concentration. These figures can be displayed interactively within the MATLAB environment, and users can also choose to save the figure as an image in various formats (e.g., PNG, JPEG, TIFF) for further analysis or reporting. Such figures may be compiled in the **figures/** directory of the code package.

7 Conclusion

This report demonstrated verification of the MATLAB-based implementation of the model developed by Mahmoudzadeh et al. (2013) for solute transport simulation through flow channels, stagnant water zones, and adjacent rock matrices. The model was used to identify canister positions experiencing dilute water concentrations that could lead to buffer erosion. The analytical solution was derived in the Laplace domain. Verification tests demonstrated excellent agreement between the MATLAB and Python implementations, with additional comparisons to the numerical model DarcyTools where applicable.

Three verification tests were carried out to assess the performance of the model under different conditions. The first test disregarded the effect of the stagnant water zone, while the second included it. Both tests confirmed that the MATLAB and Python implementations produced consistent results. The third test focused on the temporal distribution of deposition hole positions reaching three percent of the initial concentration. Once again, both implementations produced identical results, reinforcing the robustness and reliability of the model.

In addition to verifying the solute transport model, the report provides a complete description of the code package structure and workflow. This guidance enables users to modify existing cases or create new ones by altering parameters such as geometrical dimensions, transport properties, and initial and boundary conditions. The model's adaptability, coupled with the verification results, demonstrates its suitability for safety assessment calculations of radioactive waste repositories.

8 Source Code Documentation (temperate case)

8.1 PSARcalculations.m

```
% PSAR calculation: penetration of dilute water
%% Initialisations
clc; clear all; close all;
alph_in = 0; tol = 1.0e-40; % Parameters for the inverse Laplace
function
%
STWZ   = 1; % 1:STWZ will be included, 0:TWZ will be ignored
flag   = 1; % 1:Heaviside input function, 0:Pulse input function
t      = logspace(1, 9, 90);% Define logarithmic time vector(y)
C0     = 10;                % Initial concentration (g/L)
Cin    = 0.2;               % Inlet concentration (g/L)
alpha  = 0.03;              % Reduction factor from C0 to C_crit.
C_crit = alpha*C0;          % Erosion concentration (g/L)

%% Reading the input files and filtering the paths
fname  = 'Kopia av backward paths'; % read data from excel file
TW     = xlsread(fname,'Blad1','M11:M6926');
F      = xlsread(fname,'Blad1','N11:N6926');
OKFLAG = xlsread(fname,'Blad1','I11:I6926');
FPC    = xlsread(fname,'Blad1','AB11:AB6926');
EFPC   = xlsread(fname,'Blad1','AC11:AC6926');

valid_indices = OKFLAG == 0 & FPC == 0 & EFPC < 5; %Valid path
criteria

TW      = TW(valid_indices); % Filtered TW values
F       = F(valid_indices);  % Filtered F values
num_pos = length(TW);        % Number of valid positions

%% Calculating the outlet concentration profile
c = zeros(length(t), num_pos);
for j = 1:num_pos
    [dataf,datas] = BasicSetting(TW(j),F(j));
    c(:,j) =
invlap('LPsolution',t',alph_in,tol,flag,dataf,datas,C0,Cin,STWZ);
end
```

```
%% Find the positions that experience dilute water c <= C_crit
PH = c <= C_crit;      % PH(i,j)=1 if c(i,j)<= C_crit
                       % PH(i,j)=0 if c(i,j)> C_crit


% Calculate the fraction of dilute water cases
M = sum(PH, 2)/6919;
%% Plotting the calculated fraction and exporting the figure to
a png file
colorOrder = [
 0 0.4470  0.7410; % blue
 0.8500    0.3250 0.0980;   % reddish-orange
 0.9290    0.6940 0.1250;   % yellow
 0.4940    0.1840 0.5560;   % purple
 0.4660    0.6740 0.1880;   % green
 0.3010    0.7450 0.9330;   % light blue
 0.6350    0.0780 0.1840;   % dark red
 0.8       0.7 0.9 ;        % light purple
 0.6       0.9 0.6 ];       % light green
figure('Position', [100, 100, 800, 600]);
xlabel('Time (year)', 'FontSize', 14, 'FontWeight', 'bold');
ylabel('Fraction', 'FontSize', 14, 'FontWeight', 'bold');
title(['C_{0} = ', num2str(C0), ' g/L', ', \alpha = ',
num2str(alpha), ', C_{in} = ', num2str(Cin), ' g/L']);
legend('show', 'Location', 'northwest', 'FontSize', 12);
set(gca, 'XScale', 'log', 'FontSize', 12);
grid on; grid minor;
box on; hold on;
plot(t, M,'LineWidth', 2, 'DisplayName', ['C_{crit} = ',
num2str(C_crit), ' g/L'], 'Color', colorOrder(1,:));
set(gca, 'XLim', [min(t), max(t)],'YLim', [min([M(:,
1)]),max([M(:, 1)])]);
TL1 = 1e4;
TL2 = 6e4;
plot([TL1 TL1] , [0.0 max([M(:, 1)])],'LineWidth', 2, 'Color',
colorOrder(8,:), 'HandleVisibility', 'off');
hold on
plot([TL2 TL2] , [0.0 max([M(:, 1)])],'LineWidth', 2, 'Color',
colorOrder(9,:), 'HandleVisibility', 'off');
png_fname = 'Temperate.png';
saveas(gcf, png_fname);
```

8.2 BasicSetting.m

```
function [dataf,datas] = BasicSetting(TW,F)
%% define the fracture properties
Wf     = 0.1;    % fracture half-width (m)
Ws     = 1;      % stagnant water zone half-width (m)
tw     = TW;     % water residence time
FRf    = F;      % F-ratio for the fracture
Rf     = 1.0;    % retardation factor
bf     = tw/FRf;

%% define properties of matrix adjacent to the fracture
y2s    = 365*24*60*60;% year to second factor
deltaf = 12.5;        % penetration depth (m)
Def    = 4e-14*y2s;   % effective diffusivity (m^2/y)
KdfRbf = 0.0037;      % product of distribution coefficient and
bulk density

%% define the stagnant water zone properties
bs     = bf;          % fracture half-aperture (m)
Ds     = 0.0315;      % water diffusivity
Rs     = 1.0;         % retardation factor

%% define properties of matrix adjacent to the stagnant water zone
deltas = 12.5;        % penetration depth (m)
Des    = 4e-14*y2s;   % effective diffusivity (m^2/y)
KdsRbs = 0.0037;      % product of distribution coefficient and
bulk density

%% derived parameters
Daf    = Def./KdfRbf;       % apparent diffusivity for the rock
adjacent to the flow channel
MPGf   = sqrt(Def.*KdfRbf); % material property group for the
rock adjacent to the flow channel
ts     = Ws^2/Ds;           % water diffusion time
FRs    = Ws^2./(Ds.*bs);    % F-ratio for the stagnant water zone
Das    = Des./KdsRbs;       % apparent diffusivity for the rock
adjacent to the stagnant water zone
MPGs   = sqrt(Des.*KdsRbs); % material property group for the
rock adjacent to the stagnant water zone

%% setup the data
dataf = {tw,Rf,Wf,FRf,Def,Daf,deltaf,MPGf};
datas = {ts,Rs,Ws,FRs,Des,Das,deltas,MPGs};
```

8.3 LPsolution.m

```
function F = LPsolution(s,flag,dataf,datas,C0,Cin,STWZ)
%% Extract the input parameters for the fracture zone
tw  = dataf{1}; Rf  = dataf{2}; Wf  = dataf{3};    FRf  = dataf{4};
Def = dataf{5}; Daf = dataf{6}; deltaf = dataf{7}; MPGf = dataf{8};

%% Extract the input parameters for the STWZ zone
ts  = datas{1}; Rs  = datas{2}; Ws  = datas{3};    FRs  = datas{4};
Des = datas{5}; Das = datas{6}; deltas = datas{7}; MPGs = datas{8};

%% Defining the model characteristic parameters in the Laplace domain
ns = length(s);
alphaf      = zeros(ns,1);
alphas      = zeros(ns,1);
Pf          = zeros(ns,1);
Ps          = zeros(ns,1);
OMEGAf      = zeros(ns,1);
OMEGAs      = zeros(ns,1);
F           = zeros(ns,1);
alphaf(:,1) = deltaf.*sqrt(s./Daf);
Pf(:,1)     = MPGf.*tanh(alphaf(:,1));
alphas      = deltas.*sqrt(s./Das);
Ps(:,1)     = MPGs.*tanh(alphas(:,1));
OMEGAf(:,1) = Rf.* tw.* s + FRf .* Pf(:,1) .* sqrt(s);
OMEGAs(:,1) = Rs.* ts.* s + FRs .* Ps(:,1) .* sqrt(s);

%% Define the Laplace solution of the fracture-concentration
if isequal(STWZ,0); OMEGAs(:,1) = 0; end
if isequal(flag,0)
   F(:,1) = C0./s+(Cin-C0./s).*exp(-OMEGAf(:,1)-((FRf./
FRs).*(Ws./Wf)*sqrt(OMEGAs(:,1)).*tanh(2*sqrt(OMEGAs(:,1)))));
else
   F(:,1) = C0./s+((Cin-C0)./s).*exp(-OMEGAf(:,1)-((FRf./
FRs).*(Ws./Wf)*sqrt(OMEGAs(:,1)).*tanh(2*sqrt(OMEGAs(:,1)))));
end
```

Notation

b_f	Half aperture of the flow channel (L)
b_s	Half aperture of the stagnant water zone (L)
C_{in}	Concentration at the inlet of the flow channel (ML^{-3})
C_0	Initial concentration in the flow channel and matrix (ML^{-3})
C_f	Concentration in the flow channel (ML^{-3})
C_{pf}	Porewater concentration in the rock matrix adjacent to the flow channel (ML^{-3})
C_{ps}	Porewater concentration in the rock matrix adjacent to the stagnant water zone (ML^{-3})
C_s	Concentration in the stagnant water zone (ML^{-3})
D_{af}	Apparent diffusivity in the rock matrix adjacent to the flow channel (L^2T^{-1})
D_{as}	Apparent diffusivity in the rock matrix adjacent to the stagnant water zone (L^2T^{-1})
D_{ef}	Effective diffusivity in the rock matrix adjacent to the flow channel (L^2T^{-1})
D_{es}	Effective diffusivity in the rock matrix adjacent to the stagnant water zone (L^2T^{-1})
D_s	Diffusivity in the water in the stagnant water zone (L^2T^{-1})
F_f	Ratio of the flow-wetted surface of the flow channel to the volumetric flow rate (TL^{-1})
F_s	Ratio of the stagnant-water-wetted surface to the diffusion conductance of the stagnant water zone (TL^{-1})
MPG_{pf}	Material property group of the rock matrix adjacent to the flow channel ($LT^{-1/2}$)
MPG_{ps}	Material property group of the rock matrix adjacent to the stagnant water zone ($LT^{-1/2}$)
N	Ratio between the diffusion rate into the stagnant water zone and the mass flow rate through the channel (-)
R_f	Surface retardation coefficient in the flow channel (-)
R_{pf}	Retardation coefficient of the rock matrix adjacent to the flow channel (-)
R_{ps}	Retardation coefficient of the rock matrix adjacent to the stagnant water zone (-)
R_s	Surface retardation coefficient in the stagnant water zone (-)
s	Laplace transform variable (T^{-1})
t	Time (T)
u	Groundwater velocity (LT^{-1})
W_f	Half width of the flow channel (L)
W_s	Half width of the stagnant water zone (L)
x	Distance along the flow direction (L)
y	Distance into the stagnant water zone (L)
z	Distance into the rock matrix adjacent to the flow channel
z_s	Distance into the rock matrix adjacent to the stagnant water zone
δ_f	Thickness of the rock matrix adjacent to the flow channel (L)
δ_s	Thickness of the rock matrix adjacent to the stagnant water zone (L)

ε_{pf}	Porosity of the rock matrix adjacent to the flow channel (-)
ε_{ps}	Porosity of the rock matrix adjacent to the stagnant water zone (-)
τ_f	Characteristic time of advection (-)
τ_{DF}	Characteristic time of diffusion in the rock matrix adjacent to the flow channel (-)
τ_{DS}	Characteristic time of diffusion in the rock matrix adjacent to the stagnant water zone (-)
τ_s	Characteristic time of diffusion through the stagnant water zone (-)

Subscripts

f	Refers to the flow channel
s	Refers to the stagnant water zone
pf	Refers to the rock matrix adjacent to the flow channel
ps	Refers to the rock matrix adjacent to the stagnant water zone

References

SKB's (Svensk Kärnbränslehantering AB) publications can be found at www.skb.com/publications.

Bird R B, Stewart W E, Lightfoot E N, 2002. Transport phenomena, 2nd edn. Wiley, New York.

Boupha K, Jacobs J M, Hatfield K, 2004. MDL Groundwater software: Laplace transforms and the De Hoog algorithm to solve contaminant transport equations. Comput. Geosci. 30 (5), 445–453.

De Hoog F R, Knight J H, Stokes A N, 1982. An improved method for numerical inversion of Laplace transforms. SIAM J. Sci. Stat. Comput. 3 (3), 357–366.

Mahmoudzadeh B, Liu L, Moreno L, Neretnieks I, 2013. Solute transport in fractured rocks with stagnant water zone and rock matrix composed of different geological layers—model development and simulations. Water Resour. Res. 49, 1709–1727.

Moreno L, Crawford J, 2009. Can we use tracer tests to obtain data for performance assessment of repositories for nuclear waste? Hydro- Geol. J. 17, 1067–1080.

Shahkarami P, Sidborn M, 2023. Simulation of Helium transport in fractured rocks: Implementation of a dual continuum model in DarcyTools. Journal of Contaminant Hydrology, 253, 104123.

Svensson U, Kuylenstierna, H O, Ferry M, 2010. DarcyTools version 3.4 – Concepts, Methods and Equations. SKB R-07-38, Svensk Kärnbränslehantering AB.

SKB, 2022. Post-closure safety for the final repository for spent nuclear fuel at Forsmark. Radionuclide transport report, PSAR version. SKB TR-21-07, Svensk Kärnbränslehantering AB.

Arkitektkopia AB, Bromma, 2025

SKB is responsible for managing spent nuclear fuel and radioactive waste produced by the Swedish nuclear power plants such that man and the environment are protected in the near and distant future.

skb.se